COLLIMATION SYSTEM FOR BEAM LOSS LOCALIZATION WITH SLIP STACKING INJECTION IN THE FERMILAB MAIN INJECTOR*

Bruce C. Brown†, Fermilab, Batavia, IL 60510, USA

Abstract

Slip stacking injection for high intensity operation of the Fermilab Main Injector produces a small fraction of beam which is not captured in buckets and accelerated. A collimation system has been implemented with a thin primary collimator to define the momentum aperture at which this beam is lost and four massive secondary collimators to capture the scattered beam. The secondary collimators define tight apertures and thereby capture a fraction of other lost beam. The system was installed in 2007 with commissioning continuing in 2008. The collimation system will be described including simulation, design, installation, and commissioning. Successful operation and operational limitations will be described.

HIGH INTENSITY OPERATION

The Fermilab Main Injector is moving to high intensity operation[1] for production of anti-protons for the Tevatron Collider physics program and neutrinos in the NuMI[2] neutrino beamline. With a circumference of seven times that of the Fermilab Booster, stacking is required to achieve intensities beyond that provided by six Booster batches (leaving room for kicker rise times). Slip stacking injection[3][4] has been developed to allow injection of eleven Booster batches per Main Injector acceleration cycle. Figure 1 shows beam transmission and losses for a typical acceleration cycle.

Slip stack injection is implemented by transferring five Booster batches into ∼100 kV buckets in one rf system at the central injection frequency, decelerating them to a ∼1400 Hz lower frequency to leave room at the central orbit (and frequency). Five additional batches are injected into ∼100 kV buckets of a separate rf system. When circulating at the injection field but not at the central frequency, the proton bunches slip with respect to the phase of the central frequency. Beam in both systems are accelerated to symmetric offsets with respect to the central frequency. When the phase slip has placed pairs of bunches in alignment, the rf is configured to provide a single rf system and the bunches from each injection are re-captured into a ∼1 MV bucket. Finally, an eleventh Booster batch is injected into the available location.

To preserve low longitudinal emittance, the Booster intensity is limited to $\leq 4.3 \times 10^{12}$ protons/Booster batch. Nevertheless, typical beam quality (tails of longitudinal emittance) is not sufficient to permit capture and acceleration of all of the slip stacked beam. The losses from slip stacked injection[1] fall almost entirely into three categories:

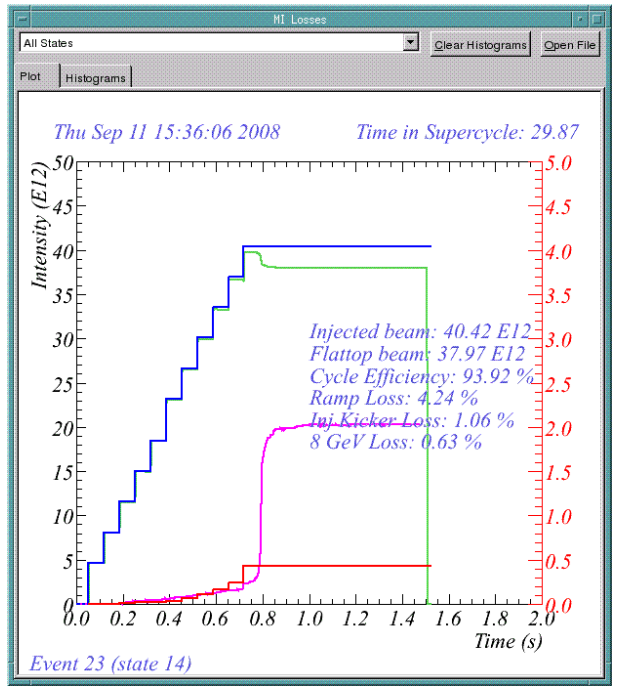

Figure 1: Beam for a typical Main Injector Cycle with 11 batch slip stack injection. The blue line shows the sum of injected beam (toroid), the green line indicates the beam intensity (DCCT), the red line indicates injected beam which is immediately lost (toroid minus change in DCCT), purple shows lost beam (DCCT). Acceleration begins at the end of injection. A major loss occurs after acceleration begins.

- Beam from previously injected batches can slip into the gap which should be preserved for the injection kicker. This beam is kicked from the circulating orbit and lost downstream of the injection kicker.

- Beam which has slipped into the extraction kicker gap can be captured by the ∼1 MV rf and accelerated to full energy. This beam is mis-steered on the rising or falling edges of the extraction kicker pulse and creates losses near the extraction point at MI52. The Main Injector transverse damping system[5] is used in anti-damping mode to 'fuzz' this beam, starting at injection energy, so as to drive it to large emittance, removing much of it at transverse apertures while still at low energy so that it will create less residual radiation.

* Operated by Fermi Research Alliance, LLC under Contract No. DE-AC02-07CH11359 with the United States Department of Energy.

† bcbrown@fnal.gov

- Beam from the slip stacking injection which is not captured within the accelerating buckets will fail to accelerate. As the magnetic field ramps up during acceleration, this beam will reach the momentum aperture of the Main Injector and be scattered to loss points around the ring. Localizing the radiation from this loss process is the principal purpose of the Main Injector Collimation System.

The Main Injector Collimation System is designed to define the momentum aperture with a primary collimator and to capture the scattered beam which strikes that collimator using secondary collimators and masks.

SIMULATION OF LOSSES AND COLLIMATION

An increase in beam loss in the Main Injector was anticipated and residual radiation survey efforts were intensified in anticipation of operation for the NuMI beam. As slip stacking injection was developed, first for anti-proton production and then for neutrino production, it became apparent that the collimation effort would need to focus on losses due to uncaptured beam. A simulation effort and collimation design study was carried out using the STRUCT tracking code and MARS energy deposition code of the Fermilab Energy Deposition Group.

Simulation

In preparation for collimator system design, a tracking simulation of the Main Injector losses was created. Attention was directed to the

- Injected beam parameters
- rf Manipulations for Slip Stacking
- Apertures of Ring Components
- Magnetic fields

Results were evaluated with particular attention to

- Time distribution of beam losses
- Pattern of losses around the ring

To achieve the observed time distribution of losses (transmission) required attention to the details of the input beam distribution and the rf manipulations. However, the resulting loss pattern showed losses only at points of high dispersion whereas slip stacking operation at that time (using two Booster batches directed to the anti-proton target) found large losses where apertures were limited at the Lambertson magnets used for beam transfer. The aperture restrictions in the Lambertson magnets are most significant in the vertical plane. The major features of the observed losses were well simulated after adding higher harmonic fields to the magnetic field description. This is

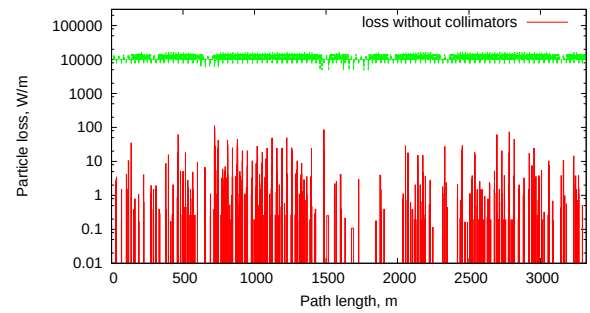

Figure 2: Particle loss distribution along the Main Injector for uncaptured beam from slip stack injection without collimation.

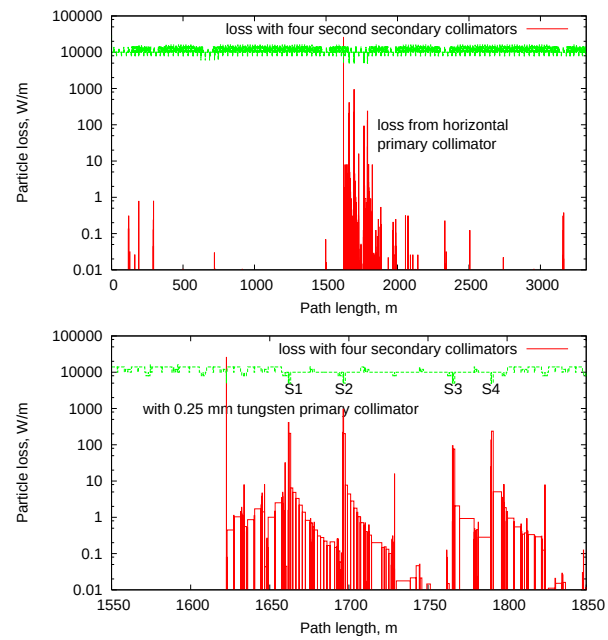

Figure 3: Particle loss distribution along the Main Injector for uncaptured beam from slip stack injection with collimation. Lower figure shows region around collimation system.

attributable to the resonant-like phenomena for large tune variations experienced by beams with large momentum error with high chromaticity settings. Significant growth of vertical emittance was predicted and observed. Figure 2 shows the loss distribution around the Main Injector simulated by STRUCT. With collimators to limit the momentum excursion of un-accelerated beam, the simulation can provide good guidance for collimator design.

Collimation Concept

The collimation concept uses a 0.25 mm Tungsten (W) primary collimator at the horizontally focusing location in a cell where dispersion has a typical value of about 1.5 m. At suitable betatron phases downstream one places large secondary collimators to absorb the beam particles which are

scattered by the primary collimator. Immediately downstream of the primary collimator and again just ahead of the next magnet one places steel masks to surround the beam pipe and intercept outscattered particles and forward shower particles. Using this design, the simulation indicated that more than 99% of the losses due to uncaptured beam could be contained in the section containing the collimators[6]. Figure 3 shows the loss simulation with collimation. Note the loss peaks for the primary collimator and four secondary collimators.

Location for Collimation

The lattice of the Main Injector consists of regular bending cells with 6-m dipoles and standard quadrupoles, dispersion suppression cells with 4-m dipoles and long quadrupoles and straight sections with no bending between quadrupoles. The FODO lattice continues through the straight sections using standard quadrupoles. Table 1 describes the uses for the straight sections. After the Recycler Ring (RR) was added to the design, all straight sections were occupied. Note also that all are used for radial transfers except for the injection at MI10. This required the design of the collimation system system to be incorporated into the MI30 straight section along with the kicker for Recycler transfers. In addition, the electron cooling system (ECOOL) which reduces the emittance of the anti-proton beam in the recycler has its cooling straight section with associated sensitive electronics in the middle of the MI30 straight section (above the Main Injector beam). The simulation indicates low losses at ECOOL which is in the region between the second and third secondary collimator in Figure 3.

Table 1: Main Injector Straight Sections

Label	**Length (Cells)**	**Use**
MI10	2	Injection
MI22	1.5	RR Transfer
MI30	4	RR Transfer Kicker Collimation
MI32	1.5	RR Transfer
MI40	2	Abort
MI52	1.5	Transfer to TeV
MI60	4	rf NuMI Extraction
MI62	1.5	Transfer to TeV

Figure 4: Examples of installed collimators: 20-Ton Secondary, steel and concrete mask (STCM), steel and marble mask (STMM) and the concrete wall are shown.

HARDWARE AND COMMISSIONING

Primary Collimator

The choice of the MI300 straight section for collimation defines the location for the primary collimator. It is placed in the last half-cell upstream of the straight section which has high dispersion. By moving three half-cells upstream to MI230, the dispersion is 1.5 m (the dispersion value for regular cells is 1.7 m). The vertical edge of a 0.25 mm tungsten (W) foil is positioned (0.001″ least count) on the radial inside of the aperture between the quadrupole and the next dipole. During acceleration, as uncaptured beam moves radially inward due to dispersion, the protons are scattered by this foil. Secondary collimators locations are selected according to the phase advance from the primary collimator. Four secondary collimators were constructed, providing good capture efficiency and some redundancy in case of failure of the positioning systems.

Secondary Collimators

To avoid the need for moving devices in the vacuum, the secondary collimators employ fixed apertures (2″ × 4″), defined by a thick-walled stainless steel vacuum box (1″ walls) connected by bellows to vacuum systems upstream and downstream. The vacuum box is surrounded by a 20-Ton steel absorber (46″ wide in horizontal direction) which contains most of the remaining hadronic shower. The aisle side, faces upstream and downstream, and aisle side of the top are covered with a 12 cm marble layer. This reduces the residual radiation exposure during tunnel access since it is minimally activated but absorbs many of the MeV gamma rays emitted from the activation products of the steel inside. This assembly is mounted on a precision motion system which provides 0.001″ least count motion with a range (±2″ × ±1″) sufficient to obscure the beam centerline.

The vacuum box is tapered on the upstream end so that the particles which are parallel to the beam centerline but strike the collimator will enter with an 18 milliradian angle. This minimizes outscatter from the shower while also placing the most intense beam energy deposition at the end of the taper which is 14″ from the upstream end. This design allows the heat to be efficiently transmitted from the stainless steel to the surrounding iron, increasing the thermal capacity of the system.

Table 2: Collimation Components

Collimation Component	Locations Employed
Primary	230
Secondary	301,303,307,308
STCM	301,303,308
STMM	301,303,308
Polyethylene	301,303,307,308
Concrete Wall	305

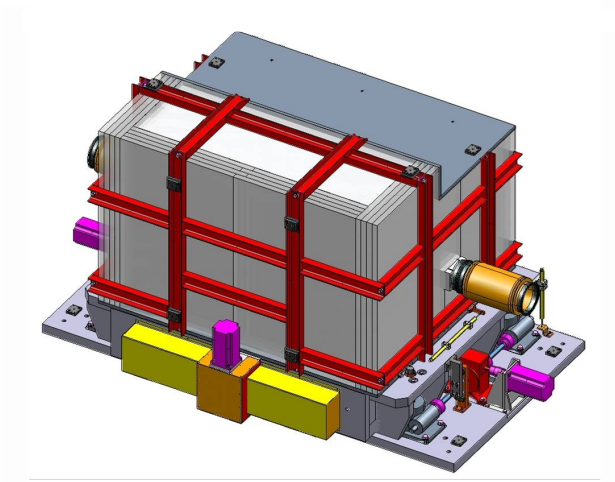

Figure 5: Design for 20-Ton Secondary Collimators as viewed from the upstream aisle side. At the upstream end we see the beam pipe bellows connecting to the collimator vacuum box. The surrounding steel is covered by four layers of 3 cm thick marble. Reduced height on wall side leaves space for magnet bus and tunnel water utilities. Motors and readout for vertical motion are upstream and downstream. Radial motion is provided from the aisle side.

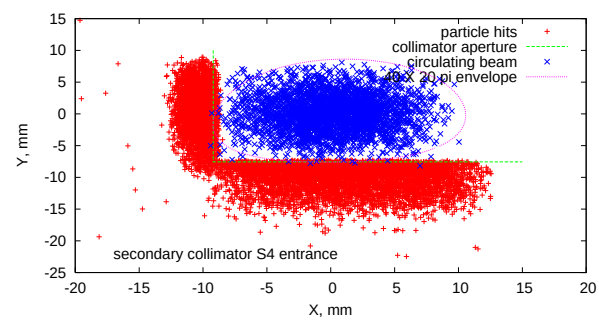

Figure 6: The corner of the collimator aperture is shown along with simulation of the circulating beam (blue - low sampling rate) along with scattered particles which strike the collimator (red - high sampling rate)

Collimation Masks

The secondary collimators are normally displaced radially and vertically inward so that the circulating beam is near a corner[6] and the particles scattered by the primary collimators strike the adjacent edges, see Figure 6. The opposite corner of the secondary collimator vacuum box is moved outward from the center, exposing downstream objects. The flux of particles which are transmitted down the beam pipe from the secondary collimators are partially intercepted by iron masks which are stacked outside of the regular beam pipe. The steel and concrete mask (STCM) placed immediately downstream of the 20-T collimators uses iron to catch beam or shower particles with concrete surrounding the iron to absorb neutrons. It blocks the aperture which is exposed by the motion of the sec-

ondary collimator just upstream and also absorbs outscatter of primary and secondary particles from the 20-T collimator. An additional mask (steel and marble mask - STMM) is placed immediately upstream of the next magnet to further absorb forward shower particles, thus protecting the accelerator components. Steel is surrounded with marble to reduce residual radiation exposure. Upstream of the ECOOL region, a wall of concrete blocks was constructed to minimize the flux of slow neutrons flowing from the first two secondary collimators toward ECOOL. A polyethylene block surrounds the stainless steel vacuum box of each primary collimator on the upstream end to attenuate the flux of neutrons which strike the upstream quadrupole. Figure 4 shows example photographs of a secondary collimator, STCM, STMM and the concrete wall. Table 2 lists the collimation components as installed. Shielding to reduce radiation damage to magnets has been added using sand and polyethylene beads where appropriate. Details of the collimation hardware are available in Beams-doc-2881[7].

Collimation Orbits

In the MI300 straight section, the horizontal orbits in the Main Injector for anti-proton beam transfer to (from) the Recycler Ring are far off center for the circulating beam at transfer time and for the first (last) turn. Figure 7 shows orbits for beam transfers from the Accumulator to the Recycler while Figure 8 shows the orbits for transfers of the cooled anti-protons from the Recycler. These orbits must be taken into account in designing orbits for collimation. Orbit distortions to permit collimation are implemented with time bumps to move the beam edge to a location where the secondary collimators can be positioned to intercept the uncaptured beam while providing a safe margin for the anti-proton transfers. The edge of the beam being collimated should be parallel to the collimator which is aligned parallel to the centerline of the MI300 straight section. An orbit which is in use (Summer 2008) is shown in Figure 9. Similar orbit considerations apply to the vertical plane but constraints from the anti-proton transfers are not significant. Since the beam envelope is either converging or diverging (depending upon location and whether horizontal or vertical), one needs to adjust the beam angle if the beam to be collimated has a larger (or smaller) emittance than has been assumed.

Collimator Transverse Positions

To confirm the fundamental assumption of the collimation design, one can examine the momentum aperture. It is determined by the relation between the position of the primary collimator and the horizontal beam position established by the local orbit time bump. Observing the loss time, as in Figure 10, and the known change in momentum as a function of primary collimator position confirms that the uncaptured beam responds to the 1.5 m dispersion as determined independently. The time required for the beam to be lost (the width of the loss vs. time) corresponds to

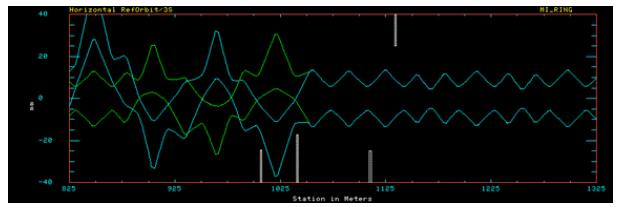

Figure 7: Horizontal orbit for anti-proton transfer from Accumulator to Recycler. The beam edge is shown for 95% emittance of 20 π mm-mr. The beam arrives from right. The "counterwave" orbit (green) is imposed by a time bump. The kicker at MI304 ($\sim$ center) transfers the beam with the blue orbit with the extraction point at the peak on the left. Positions for C301 and C303 and the primary collimator are limited to avoid these beam edges.

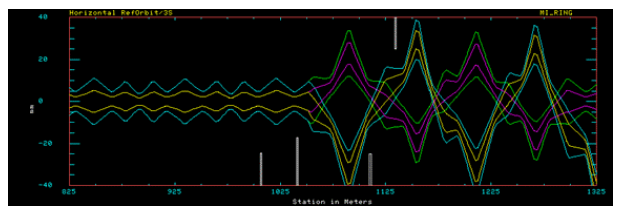

Figure 8: Horizontal orbit for anti-proton transfer from Recycler to Tevatron. The beam edge (yellow or purple) is shown for the expected 3 π mm-mr beam from the Recycler. Also shown (blue or green) are edges for 95% emittance of 10 π mm-mr. The beam arrives from the injection point on the right with the yellow (blue) edges. The kicker at MI304 (center) transfers the beam to the circulating orbit. To the right of the kicker, the "counterwave" orbit (purple or green) has been imposed by a time bump. Positions for C307 and C308 are limited to avoid the 10 π mm-mr beam edges providing a margin for the most important anti-proton transfers.

the known emittance and the beta functions at MI230. The beam position currently in use exposes three to six mm of the tungsten foil and sets the orbit offset at -15 mm.

Once the time bump for the collimation region orbit has been established and the position for the primary collimator is set, one needs to find suitable positions for the secondary collimators. One might expect to track the scattered beam from the position at the primary collimator as a guide for secondary collimator placement. Simulation is dependent on fine details of dispersion and betatron orbits and direct measurement is difficult. The technique employed has been to measure loss monitor response as a function of collimator displacement (horizontal and vertical) at various primary collimator locations. The time profile of losses are examined with attention to losses before and during the time when uncaptured beam loss is observed. Integrated losses are recorded a few milliseconds after the loss of uncaptured beam. Figure 11 shows a plot for the horizontal position of the first secondary collimator. Since the dispersion is very small at the collimator, the effects of vari-

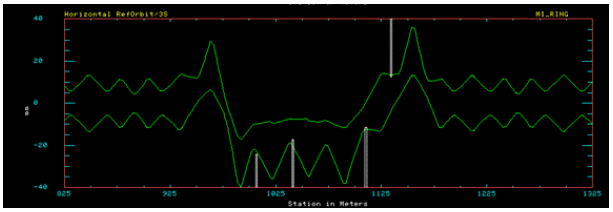

Figure 9: Horizontal Orbit for collimation. Beam edges (green) are shown for 95% emittance of 20 π mm-mr. Protons arrive from the right. The orbit is imposed as a time bump after injection to be at constant value when uncaptured beam is lost. It is designed to place the edge as shown parallel to the collimator edge (which is parallel to the centerline of the straight section). Collimator radial positions (white) are not final.

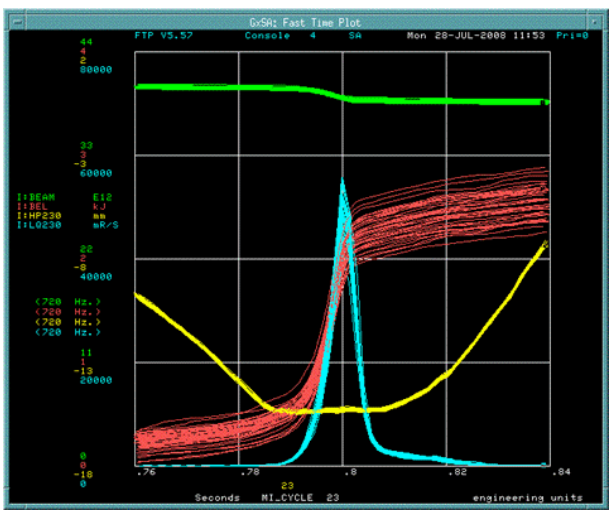

Figure 10: The time profile of losses (LQ230) due to the primary collimator are shown in blue. The green line shows beam intensity (DCCT). Beam position at the primary collimator (HP230) is shown in yellow. The beam energy loss (DCCT change times energy) is in red. Changes in the radial position of the primary collimator result in moving the time of this loss.

ous primary collimator positions will be more subtle than the changes created in the time profile by moving the primary collimator with respect to the beam edge. The lower image in Figure 11 is made with the primary collimator edge 2.5 mm nearer to the beam centerline. Efforts to optimize the collimator positions continues at this time (Summer 2008).

LOSS MEASUREMENTS AND RESULTS

The Main Injector is instrumented with Beam Loss Monitors (BLM) based on gas filled glass tubes[8]. Upgraded electronics[9] has been in use since 2007 and display applications are being upgraded. Typically, a BLM is placed on the outside tunnel wall above beam height at the downstream end of each MI Quadrupole. Additional BLM's are installed near the transfer points to aid tune-up and provide monitoring of losses on Lambertson magnets. We would note that precisely relating loss monitor readings to beam loss is complicated by many geometrical factors so the loss displays provide only guidance, not precise loss values. This system has proven its value in commissioning the Main Injector Collimation System. The electronics accumulates the loss thru the cycle and it can be stored at 'PROFILE' times defined externally. The loss can be integrated on two shorter time scales for sampling or plotting. Figure 10 shows the fast loss for the LM230 monitor.

A program to read and display the array of losses at 'PROFILE' times has been developed. The data for a cycle

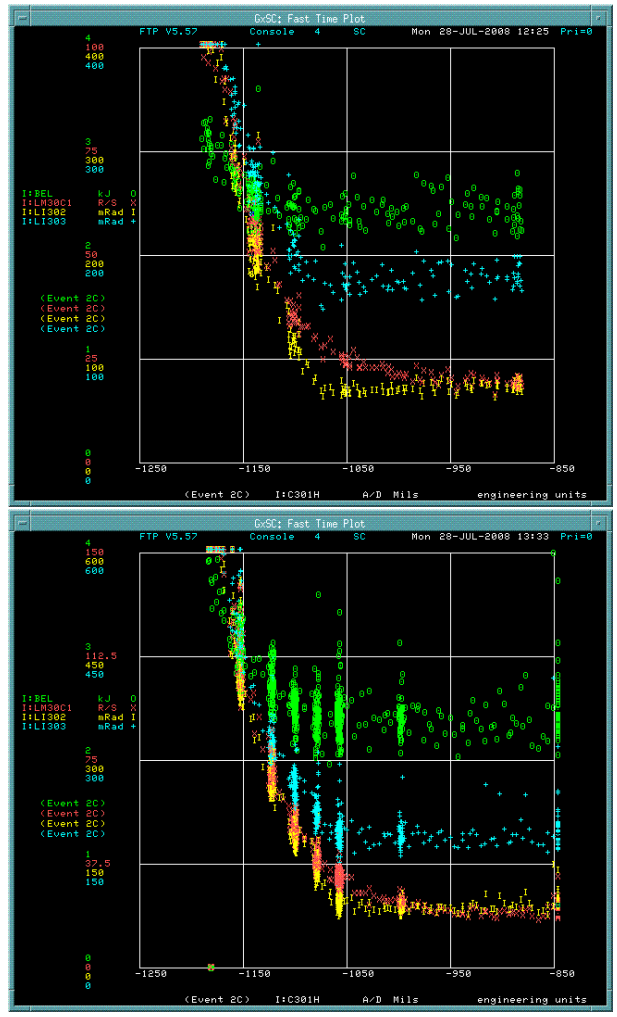

Figure 11: Scan of loss vs. horizontal position for the first secondary collimator (C301). Green indicates the loss of accelerated beam current. Red shows loss at loss monitor on beam pipe downstream of C301. Yellow and Blue indicate losses measured with loss monitors at Q302 and Q303. Upper image is scan with primary at 600 mil reading; lower image is scan with primary at 700 mil reading. Note that the collimator has captured significant loss before the transmission is reduced.

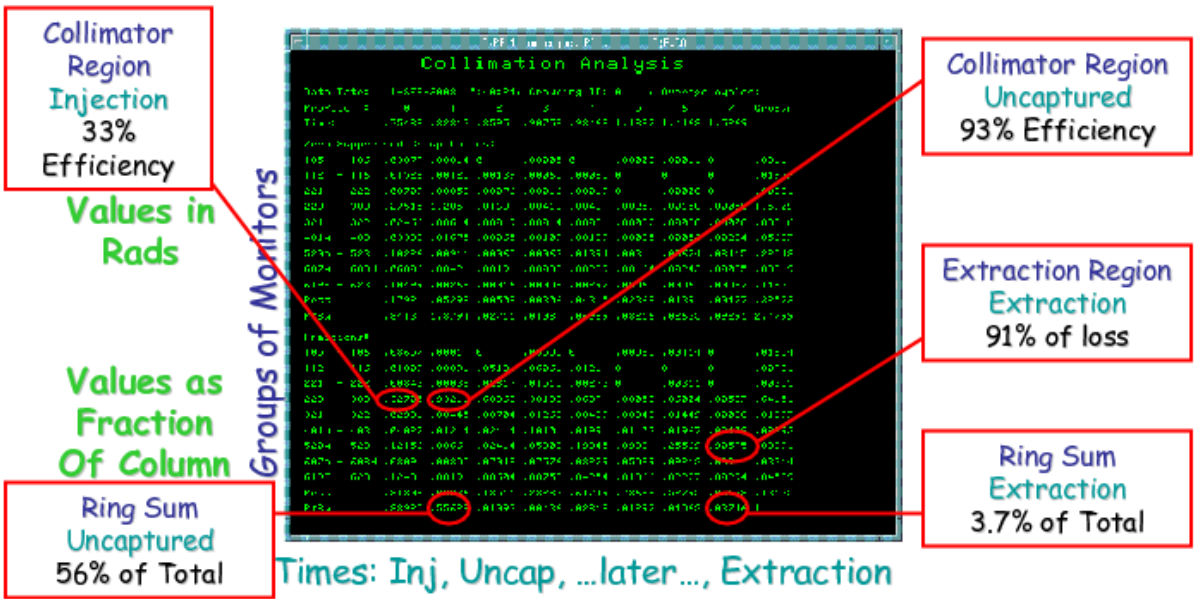

Figure 12: Summary of losses by BLM group and time. Rows give loss summarized by group where the losses are those integrated between 'PROFILE' times (columns). The annotation boxes are labeled with the BLM group above, the 'PROFILE' time, and the value.

can be stored in a database for evaluation later or displayed in summary form to aid in tuning. The display is annotated to create Figure 12. The data is displayed in an array where columns correspond to 'PROFILE' times. Rows show sums for groups of adjacent loss monitors. In the section just below the header information, the integrated loss differences from the previous column are shown. The sum around the ring for that data follows. A sum for the row appears in the last column with a ring total in the sum row. This data is expressed in units of rads per cycle impinging on the standard loss monitor. Below that the data are displayed as a fraction of the sum, first for each time slot and loss monitor group. Again, the bottom row shows the fraction of the total in each time slot while the last column shows the loss fraction in each monitor group.

For the data in Figure 12, the 4th loss group row (from 229 to 309) is the collimation region. 'PROFILE' times have been set to record the losses from uncaptured beam in the second time column. Looking the the fractional display section we see that 92% of the ionization in this time slice is in the collimation region. The first profile is taken at the end of the injection and we see that 34% of those losses are also in the collimation region. Other groups or profile times can be employed.

A more complete visual display is provided as shown in Figure 13. Each loss monitor around the ring is shown sequentially, starting at the injection region. On a a three-decade log scale, the integrated loss at the end of the cycle is plotted in green. It is overplotted in yellow with the integrate losses at the profile time just after the loss of uncaptured beam. Finally, this is overplotted in blue with losses at the end of the injection process. This display is provided in the control room at all times to allow continuous observation of the collimation effects. On the bottom of the display, the sums (in rads/pulse) for the end of cycle (green) for the ring sum and the collimator region, for the collimator region at injection (blue) and sum and the fractional sum (93% collimator efficiency) for uncaptured beam time in the collimator region. The header includes beam intensity and transmission information (94.7% of injection beam accelerated to extraction) as well as operating state and time stamp. The data shown are typical of current operation.

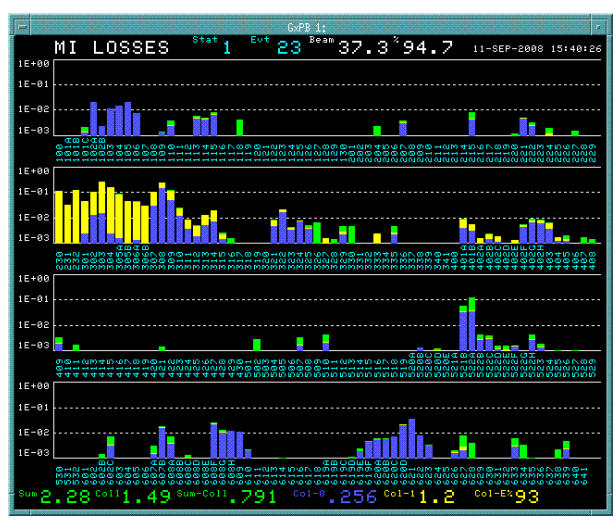

Figure 13: Loss Display for operational monitoring of collimator effectiveness.

CONCLUSION

The Collimation System at the Fermilab Main Injector has been installed and commissioned. The radiation from loss of uncaptured beam created by the slip stacking injection process are well localized with more than 90% of the measured loss occuring within the pre-defined collimator region (from the primary collimator to the end of the MI300 straight section). Much of the remaining loss is in the adjacent region downstream of the straight section. The collimators also define limiting apertures for injected beam and $>$30% of the ionization from loss of beam before acceleration is also captured in the collimator region. Other regions of the Main Injector tunnel have experienced significant reduction in activation, including a reduction in the region of the abort at MI40 where construction activities are planned. The localization predicted by the simulation effort has not yet been achieved and further tuning and studies are continuing.

ACKNOWLEDGMENTS

The author is indebted to many people. The Main Injector Group of the Fermilab Accelerator Division has been involved in all aspects of this with special thanks to Ioanis Kourbanis who has provided inspiration and helped to maintain focus. The simulation effort included calculations by Alexandre Drozhdin and Igor Rakhno with guidance from David Johnson, Nikolai Mokhov and Main Injector staff. The mechanical design was carried out by Vladimir Sidorov while Maurice Ball guided an effort to re-route bus work and utilities from the collimator locations. John Featherstone supervised the installation effort. The assistance of the Accelerator Operations group is also greatly appreciated.

REFERENCES

[1] Ioanis Kourbanis. Fermilab Main Injector High Power Operation and Future Plans. In Charlie Horak, editor, *Proceedings of the 42nd ICFA Advanced Beam Dynamics Workshop on High-Intensity, High-Brightness Hadron Beams - 2008*, Nashville, TN, USA, 2008.

[2] Sam Childress. The NuMI Beam at Fermilab: Successes and Challenges. In Charlie Horak, editor, *Proceedings of the 42nd ICFA Advanced Beam Dynamics Workshop on High-Intensity, High-Brightness Hadron Beams - 2008*, Nashville, TN, USA, 2008.

[3] K. Seiya et al. Multi-batch slip stacking in the Main Injector at Fermilab. In C. Petit-Jean-Genaz, editor, *Proceedings of the 2007 PARTICLE ACCELERATOR CONFERENCE*, pages 742–744. IEEE, Piscataway, N.J. 08855-1331, 2007. Also available as FERMILAB-CONF-07-275-AD.

[4] K. Seiya et al. Slip stacking. In W. Scandale and F. Zimmermann, editors, *PROCEEDINGS BEAM'07 CARE-HHH-APD Workshop on Finalizing the Roadmap for the Upgrade of the CERN and GSI Accelerator Complex*, page 66, Geneva, Switzerland, OCTOBER 2007.

[5] W. J. Ashmanskas et al. Operational Performance of a Bunch by Bunch Digital Damper in the Fermilab Main Injector. In C. Horak, editor, *Proceedings of the 2005 PARTICLE ACCELERATOR CONFERENCE*, pages 1440–1442. IEEE, Piscataway, N.J. 08855-1331, 2005. Also available as FERMILAB-CONF-05-145-AD.

[6] Alexandr I. Drozhdin et al. Collimation System Design for Beam Loss Localization with Slipstacking Injection in the Fermilab Main Injector. In C. Petit-Jean-Genaz, editor, *Proceedings of the 2007 PARTICLE ACCELERATOR CONFERENCE*, page 1688. IEEE, Piscataway, N.J. 08855-1331, 2007. Also available as FERMILAB-CONF-07-249-AD.

[7] Bruce C. Brown. Main Injector Collimation System Hardware. Beams-doc 2881 v2, Fermilab, April 2008.

[8] R.E. Shafer et al. The Tevatron Beam Position and Beam Loss Monitoring Systems. In Francis T. Cole and Rene Donaldson, editors, *Proceedings of the 12th International Conference On High-Energy Accelerators*, pages 609–615. Fermilab, 1983. Also available as FERMILAB-CONF-83-112-E.

[9] Al Baumbaugh et al. BLM Upgrade Users' Guide. Beams-doc 1410 v8, Fermilab, January 2008.